Noise Spectral of GML Noise and GSR Behaviors for FGLE with Random Mass and Random Frequency

Lini Qiu, Guitian He *, Yun Peng, Hui Cheng and Yujie Tang

College of Mathematics and Physics, Center for Applied Mathematics of Guangxi Minzu University, Nanning 530006, China

* Correspondence: heguitian100@163.com

Abstract: Due to the interest of anomalous diffusion phenomena and their application, our work has widely studied a fractional-order generalized Langevin Equation (FGLE) with a generalized Mittag–Leffler (GML) noise. Significantly, the spectral of GML noise involving three parameters is well addressed. Furthermore, the spectral amplification (SPA) of an FGLE has also been investigated. The generalized stochastic resonance (GSR) phenomenon for FGLE only influenced by GML noise has been found. Furthermore, material GSR for FGLE influenced by two types of noise has been studied. Moreover, it is found that the GSR behaviors of the FGLE could also be induced by the fractional orders of the FGLE.

Keywords: fractional generalized Langevin equation; GML noise; trichotomous noise; stochastic resonance

1. Introduction

Many physical systems are immersed in noisy environments. Furthermore, new order induced by noise attracts significant attention. One of the effects of noise is stochastic resonance (SR) which was coined by Roberto Benzi [1] to account for the glaciation phenomena. The SR theory has been extensively studied in various fields, including communication devices, chemical reactions, and material–physics phenomena [1–9]. SR phenomena both in nonlinear and linear systems could be induced by noise [10–15]. The traditional SR indicates that it itself exhibits maximal value for signal-to-noise ratio (SNR) versus noise intensity [1,3]. Subsequently, the generalized stochastic resonance (GSR) [10] is widely studied. In this work, we will address spectral amplification (SPA) [11–13] to describe the SR phenomena.

R. Brown discovered the Brownian motion for small pollen particles suspended in water. The diffusion, used in many branches of physics in recent decades [16,17], is described by the mean squared displacement (MSD). The scaling law $\langle x^2(t) \rangle \sim t$ is characteristic of normal diffusion, while $\langle x^2(t) \rangle \sim t^\alpha$ exhibits anomalous diffusion [17]. One should distinguish subdiffusion for $0 < \alpha < 1$ and superdiffusion for $1 < \alpha < 2$ [17]. Recently, anomalous diffusion phenomena are receiving considerable attention.

There are several approaches for describing the diffusion process. The stochastic harmonic oscillator is one of the cornerstones of statistical models and it describes stochastic systems by using Newton's second law [17,18]. Kubo coined the fluctuation–dissipation relation (FDR) to establish a relation between the thermal noise and friction forces [19]. In this condition, the diffusion process could be governed by a generalized Langevin equation (GLE) [14,15,20]. Subsequently, the subject of the GLE attracts more and more attention [14,15,20].

Fractional Calculus (FC) is a useful tool for modeling a variety of natural phenomena, involving areas in engineering, biology, finance, economy, and chemistry [21]. Additionally, a fractional Langevin equation was introduced to study anomalous diffusion [22]. Recently, the fractional-order generalized Langevin equations (FGLEs) were studied to discuss the anomalous diffusion [23,24].

Anomalous diffusion for a Brownian particle with unit mass $m = 1$ in viscoelastic media subjected to a intrinsic noise $F(t)$ could be characterized by the FGLE [23,24]:

$$_C D_0^\mu v(t) + \int_0^t \gamma(t - u)\dot{x}(u)\mathrm{d}u + U(x) = F(t), \quad _C D_0^\nu x(t) = v(t). \tag{1}$$

in which $x(t)$ denotes the displacement and $v(t)$ stands for the velocity. $U(x)$ in Equation (1) denotes a general external force. For harmonic force with free noise, $U(x)$ is written as $U(x) = \omega_0^2 x$. For harmonic force with noise, $U(x)$ can be defined as $U(x) = \omega_0^2(1 + \xi(t))x$, where $\xi(t)$ stands for an external noise, and ω_0 presents a inherent frequency. Furthermore, $\gamma(t)$ in Equation (1) is related to the intrinsic noise $F(t)$, which is zero-centered and satisfies FDR [19],

$$\langle F(t)F(u)\rangle = C(|t - u|) = \kappa_B T \gamma(|t - u|), \tag{2}$$

in which T represents the absolute temperature and κ_B signifies the Boltzmann constant.

Recently, the correlation function with a power–law correlation function was studied to investigate anomalous diffusion phenomena [14,15,25]. Most recently, a Mittag–Leffler (ML) noise was studied to address anomalous diffusion phenomena [26]. One-parameter ML correlation function $\frac{C_0}{\tau^\alpha} E_\alpha[-(\frac{|t-u|}{\tau})^\alpha]$ is used [26], where α stands for the memory exponent ($0 < \alpha < 2$), τ denotes the memory time, C_0 is a proportionality coefficient, and function $E_\alpha(s)$ denotes the ML function. Subsequently, Camargo [27] and Fa [28] studied an FGLE with a two-parameter ML function $\frac{C_0}{\tau^\alpha}|t - u|^{\beta-1} E_{\alpha,\beta}[-(\frac{|t-u|}{\tau})^\alpha]$, where the $E_{\alpha,\beta}(s)$ function denotes the two-parameter ML function. In recent papers [29], a three-parameter ML correlation function $\frac{C_0}{\tau^{\alpha\delta}}|t - u|^{\beta-1} E_{\alpha,\beta}^\delta[-(\frac{|t-u|}{\tau})^\alpha]$ was investigated to model anomalous diffusion phenomena. The three-parameter ML function, proposed by Prabhakar [30], can be reduced to various types of ML function for special parameters. Hence, three-parameter ML noise can recover for various types of ML noise, including fractional noise with power–law correlation functions and Gaussian white noise. Thus, due to its potential application in modeling anomalous diffusion, generalized Mittag–Leffler (GML) noise is becoming an intriguing subject of research.

The fluctuating parameters of the systems could be characterized by extrinsic multiplicative noise if the physical system fluctuated by external origin. Several stochastic harmonic oscillators with fluctuating parameters have been widely investigated [31]. Especially, material results of SR phenomena in stochastic harmonic oscillators have been extensively studied. For instance, the SR phenomena of stochastic harmonic oscillators with multiplicative noise were investigated [31]. Most recently, the SR phenomena in stochastic harmonic oscillators with fluctuating inherent frequency and random damping were also extensively studied [32]. Mankin and collaborators [33] introduced a trichotomous noise to describe the telegraph process. Due to the trichotomous noise including Gaussian white noise and dichotomous noise, trichotomous noise is better suited to address natural fluctuations [33]. Thus, GSR phenomena for Langevin equation with trichotomous noise attract significant attention [11]. The papers [29] have studied fractional dynamics and the statistical property of an FGLE with GML noise; however, the impact of multiple multiplicative trichotomous noise was not discussed in these systems. Due to the influence of some biological and chemical environments, the molecules of viscoelastic media are capable of both adhering and colliding to it randomly, which leads to the random mass. On the other hand, random inherent frequency may be influenced by external fluctuations, which arises from fluctuations of the potential energy. Therefore, the synergy between random mass, random inherent frequency, and GML noise should be considered. Thus, the main work is to investigate the GSR phenomena for an FGLE with multiple multiplicative trichotomous noise and a GML noise, which is missing in the literature reports. Especially, the GSR phenomenon of the FGLE only induced by a GML noise will be studied. One of the main aims of this work is to address the dynamical behavior of the various non-monotonic GSR phenomena of SPA versus the parameters of the intrinsic noise, multiplicative trichotomous

noise, and driving frequency. It is worth noting that the spectral of GML noise would be addressed due to its spectra describing the power of the noise.

2. Three-Parameter GML Noise

The noise spectral is a significant index, which describes the power of noise. The spectral of ML noise involving a one-parameter ML correlation function is studied in Ref. [34]. The three-parameter ML correlation function is written as [29]

$$\langle F(t)F(u)\rangle = C(|t-u|) = \frac{C_0}{\tau^{\alpha\delta}}|t-u|^{\beta-1}E_{\alpha,\beta}^{\delta}[-(\frac{|t-u|}{\tau})^{\alpha}], \tag{3}$$

where C_0 denotes a proportionality coefficient, $\alpha > 0, \beta > 0, \delta > 0$. The $E_{\alpha,\beta}^{\delta}(s)$ is a three-parameter ML function defined by the following series:

$$E_{\alpha,\beta}^{\delta}(s) = \sum_{k=0}^{\infty}\frac{(\delta)_k}{\Gamma(\beta+\alpha k)}\frac{s^k}{k!}, \tag{4}$$

where $(\delta)_k = \frac{\Gamma(\delta+k)}{\Gamma(\delta)}$, and $\Gamma(\cdot)$ denotes the gamma function. For $\delta = 1$, the correlation function (3) recovers to the two-parameter ML correlation function of GML noise given by

$$\langle F(t)F(u)\rangle = \frac{C_0}{\tau^{\alpha}}|t-u|^{\beta-1}E_{\alpha,\beta}[-(\frac{|t-u|}{\tau})^{\alpha}], \tag{5}$$

where the $E_{\alpha,\beta}(z)$ is a two-parameter ML function given by

$$E_{\alpha,\beta}(s) = \sum_{k=0}^{\infty}\frac{s^k}{\Gamma(\beta+\alpha k)}, \alpha > 0, \beta > 0. \tag{6}$$

For $\delta = 1, \beta = 1$, the function (3) recovers to the correlation function of ML noise with one-parameter ML function given by

$$E_{\alpha}(s) = \sum_{k=0}^{\infty}\frac{s^k}{\Gamma(1+\alpha k)}, \alpha > 0. \tag{7}$$

For $\delta = 1, \beta = 1, \alpha = 1$, $C(t)$ in Equation (3) recovers to $C(t) = \frac{C_0}{\tau}e^{-\frac{|t|}{\tau}}$, which is the function of the Ornstein–Uhlenbeck noise. For $\delta = 1, \beta = 1$ and $\tau \to 0$, the function (3) recovers to $C(t) = C_0\frac{t^{-\alpha}}{\Gamma(1-\alpha)}$, which corresponds to a power–law function. For $\delta = 1, \beta = 1$, $\alpha = 1$ and $\tau \to 0$, the function (3) recovers to $C(t) = C_1\delta(t)$, a Dirac delta function of white noise.

Taking the Laplace transform (LT) of $C(t)$, one can have

$$\hat{C}(s) = \frac{C_0}{\tau^{\alpha\delta}}\frac{s^{\alpha\delta-\beta}}{(s^{\alpha}+\tau^{-\alpha})^{\delta}}. \tag{8}$$

Assuming $\omega > 0$, after some algebra, one can yield

$$\tilde{C}(\omega) = \hat{C}(s = -i\omega) = \frac{C_0}{\tau^{\alpha\delta}}\omega^{\alpha\delta-\beta}\frac{\cos[\frac{\pi}{2}(\alpha\delta-\beta)-\varphi_1\delta]-i\sin[\frac{\pi}{2}(\alpha\delta-\beta)-\varphi_1\delta]}{[\omega^{2\alpha}+\tau^{-2\alpha}+2\omega^{\alpha}\tau^{-\alpha}\cos(\frac{\pi}{2}\alpha)]^{\frac{\delta}{2}}}, \tag{9}$$

where $\varphi_1 = \arctan\frac{\omega^{\alpha}\sin(\frac{\pi}{2}\alpha)}{\omega^{\alpha}\cos(\frac{\pi}{2}\alpha)+\tau^{-\alpha}}$.

Therefore, one has, in particular

$$\mathcal{R}e\tilde{C}(\omega) = \frac{C_0}{\tau^{\alpha\delta}} \frac{\omega^{\alpha\delta-\beta}\cos[\frac{\pi}{2}(\alpha\delta-\beta)-\varphi_1\delta]}{[\omega^{2\alpha}+\tau^{-2\alpha}+2\omega^{\alpha}\tau^{-\alpha}\cos(\frac{\pi}{2}\alpha)]^{\frac{\delta}{2}}}, \quad \omega > 0, \tag{10}$$

where $\mathcal{R}e\tilde{C}(\omega)$ denotes the real part of $\tilde{C}(\omega)$.

Thus, one can obtain the noise spectral $\langle|F(\omega)|^2\rangle$ of three-parameter ML noise,

$$\langle|F(\omega)|^2\rangle = 2\frac{C_0}{\tau^{\alpha\delta}} \frac{|\omega|^{\alpha\delta-\beta}\cos[\frac{\pi}{2}(\alpha\delta-\beta)-\varphi_1\delta]}{[|\omega|^{2\alpha}+\tau^{-2\alpha}+2|\omega|^{\alpha}\tau^{-\alpha}\cos(\frac{\pi}{2}\alpha)]^{\frac{\delta}{2}}}. \tag{11}$$

For $\delta = 1$, Equation (11) recovers to

$$\begin{aligned}
\langle|F(\omega)|^2\rangle &= 2\frac{C_0}{\tau^{\alpha}}|\omega|^{\alpha-\beta} \frac{\cos[\frac{\pi}{2}(\alpha-\beta)-\varphi_1]}{[|\omega|^{2\alpha}+\tau^{-2\alpha}+2|\omega|^{\alpha}\tau^{-\alpha}\cos(\frac{\pi}{2}\alpha)]^{\frac{1}{2}}} \\
&= \frac{2C_0|\omega|^{\alpha-\beta}\{\cos[\frac{\pi}{2}(\alpha-\beta)]+(\tau|\omega|)^{\alpha}\cos(\frac{\pi}{2}\beta)\}}{1+2(\tau|\omega|)^{\alpha}\cos(\frac{\pi}{2}\alpha)+(\tau|\omega|)^{2\alpha}}.
\end{aligned} \tag{12}$$

For $\beta = 1$ and $\delta = 1$, Equation (11) recovers to

$$\langle|F(\omega)|^2\rangle = \frac{2C_0|\omega|^{\alpha-1}\sin(\frac{\pi}{2}\alpha)}{1+2(\tau|\omega|)^{\alpha}\cos(\frac{\pi}{2}\alpha)+(\tau|\omega|)^{2\alpha}}, \tag{13}$$

which agrees with the result provided in Ref. [34].

Based on the expression spectral (11), Figure 1 exhibits a frequency-dependent spectrum of three-parameter ML noise with $C_0 = 5.52 \times 10^{-18}$ and other parameters explained in Figure 1. Figure 1a showing the spectrum for various α is monotonic decreasing for $\alpha \leq 1$, while the spectrum exhibits non-monotonicity for $\alpha > 1$. Figure 1b depicts the spectrum which presents monotonic decreasing for $\beta \leq 1$. Figure 1c plots the spectrum exhibiting monotonic decreasing for approximately $\delta < 0.5$, while the spectrum exhibits monotonic increasing for approximately $\delta > 0.5$. Figure 1d displays the monotonic decreasing spectrum for $\tau \leq 1$. One can find that the spectrum of three-parameter ML noise exhibits many characteristics. As depicted in Figure 1, for special parameters, one can find that an increasing spectrum with decreasing frequency identifies with the spectrum of $1/f$ noise or the spectrum of random carriers in lattice defects.
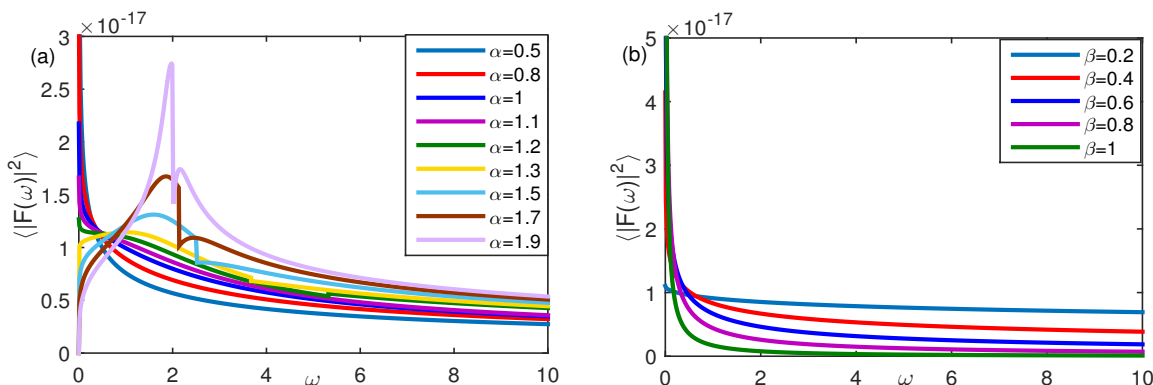
Figure 1. *Cont.*
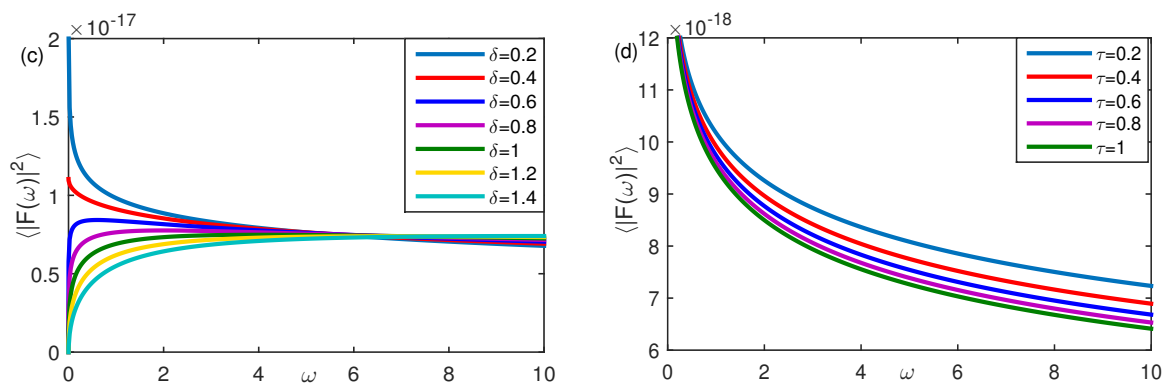
Figure 1. Spectrum of three-parameter ML noise. (**a**) Various α with $\beta = 0.5, \delta = 0.4, \tau = 0.5$; (**b**) various β with $\alpha = 0.5, \delta = 0.4, \tau = 0.5$; (**c**) various δ with $\alpha = 0.5, \beta = 0.2, \tau = 0.5$; (**d**) various τ with $\alpha = 0.5, \beta = 0.2, \delta = 0.2$.

3. FGLE with Multiplicative Trichotomous Noise

For convenience, some calculus definitions are given as follows. The Riemann–Liouville integral is written as [21]

$$I_0^p f(t) = \frac{1}{\Gamma(p)} \int_0^t (t-\varsigma)^{p-1} f(\tau) \mathrm{d}\varsigma, \ t > 0, \ p > 0. \tag{14}$$

Fractional derivatives in Caputo type is given by [21]

$$_C D_0^\mu f(t) = I^{m-\mu} f^{(m)}(t), \ \mu > 0, \ m = [\mathcal{R}e(\mu)] + 1. \tag{15}$$

One knows that external fluctuations may often connect with fluctuating parameters. Usually, the mass and inherent frequency are often immersed in the same environment. Based on the previous description, the fluctuating parameters are established by multiplicative trichotomous noise, and the thermal noise is established by a GML noise. Thus, an FGLE with random mass, random frequency, and a GML noise can be characterized by

$$(1 + \xi(t))_C D_0^\mu v(t) + \int_0^t \gamma(t-u)v(u)\mathrm{d}u + \omega_0^2(1 + \xi(t))x = A_0 \cos(\Omega t) + F(t),$$
$$_C D_0^\nu x(t) = v(t), \tag{16}$$

where ω_0 is the inherent frequency, and Ω, A_0 are the frequency and the amplitude of the external force $A_0 \cos(\Omega t)$, respectively. $\gamma(t)$ satisfies Equation (2). The thermal noise $F(t)$ is a three-parameter GML noise [29], zero-centered, meeting Equations (2) and (3). Then, $\gamma(t)$ is given by

$$\gamma(t) = \frac{C_0}{\kappa_B T \tau^{\alpha\delta}} t^{\beta-1} E_{\alpha,\beta}^\delta [-(\frac{t}{\tau})^\alpha]. \tag{17}$$

$_C D_0^\mu$ and $_C D_0^\nu$ in Equation (16) are fractional derivatives in Caputo type, $0 < \mu \leq 1$ and $0 < \nu \leq 1$. For $\nu \neq 1$, $_C D_0^\nu x$ denotes fractional velocity [12,23]. For $\nu = 1$, $_C D_0^\nu x$ recovers to ordinary velocity.

The multiplicative extrinsic noise $\xi(t)$ in Equation (16) is established by trichotomous noise [33]. Due to different origins, $\xi(t)$ and $F(t)$ are assumed to be independent, i.e., $\langle \xi(t)F(t) \rangle = 0$. The trichotomous noise $\xi(t)$ takes three values: $\pm a$ and 0, which meets $p_s(a) = p_s(-a) = q$, $p_s(0) = 1 - 2q$ for $0 < q \leq \frac{1}{2}$. Furthermore, $\xi(t)$ also meets

$$\langle \xi(t) \rangle = 0, \langle \xi(t+\epsilon)\xi(t) \rangle = 2qa^2 e^{-\lambda\epsilon}. \tag{18}$$

4. Spectral Amplification of FGLE

It is well established that the Shapiro–Loginov formula (SLF) [35] plays a significant role to solve a stochastic differential equation.

To obtain the first moment of Equation (16), it is necessary to average Equation (16), and one obtains

$$_CD_0^\mu\langle v(t)\rangle = -\langle\xi(t)_CD_0^\mu v(t)\rangle - \int_0^t \gamma(t-u)\langle v(u)\rangle\mathrm{d}u - \omega_0^2(\langle x(t)\rangle + \langle\xi(t)x(t)\rangle) + A_0\cos(\Omega t),$$

$$_CD_0^\nu\langle x(t)\rangle = \langle v(t)\rangle. \tag{19}$$

Multiplying Equation (16) by $\xi(t)$, we could also obtain

$$\langle\xi(t)_CD_0^\mu v(t)\rangle = -\langle\xi^2(t)_CD_0^\mu v(t)\rangle - \int_0^t \gamma(t-u)\langle\xi(t)v(u)\rangle\mathrm{d}u - \omega_0^2(\langle\xi(t)x(t)\rangle + \langle\xi^2(t)x(t)\rangle),$$

$$\langle\xi(t)_CD_0^\nu x(t)\rangle = \langle v(t)\xi(t)\rangle. \tag{20}$$

To split two correlators $\langle\xi(t)_CD_0^\nu x(t)\rangle$ and $\langle\xi(t)_CD_0^\mu v(t)\rangle$, one can exploit the definition of fractional calculus and the Shapiro–Loginov procedure, and we can yield

$$\langle\xi(t)_CD_0^\mu v(t)\rangle = e^{-\lambda t}\,_CD_0^\mu[\langle v(t)\xi(t)\rangle e^{\lambda t}],$$

$$\langle\xi(t)_CD_0^\nu x(t)\rangle = e^{-\lambda t}\,_CD_0^\nu[\langle x(t)\xi(t)\rangle e^{\lambda t}]. \tag{21}$$

For the new correlator $\langle\xi(t)v(u)\rangle$, after using the SLF procedure, we yield

$$\langle v(u)\xi(t)\rangle = \langle v(u)\xi(u)\rangle e^{-\lambda(t-u)} \tag{22}$$

Equation (20) contains the high-order correlator $\langle\xi^2(t)_CD_0^\mu v(t)\rangle$, and one has to use a decoupling procedure. Multiplying Equation (16) by $\xi^2(t)$, using $\xi^3(t) = a^2\xi(t)$ and $\langle\xi^2(t)\rangle = 2qa^2$, after averaging one can yield

$$\langle\xi^2(t)_CD_0^\mu v(t)\rangle + a^2\langle\xi(t)_CD_0^\mu v(t)\rangle + \int_0^t \gamma(t-u)\langle\xi^2(t)v(u)\rangle\mathrm{d}u + \omega_0^2(\langle\xi^2(t)x(t)\rangle$$

$$+ a^2\langle\xi(t)x(t)\rangle) = 2qa^2A_0\cos(\Omega t),$$

$$\langle\xi^2(t)_CD_0^\nu x(t)\rangle = \langle\xi^2(t)v(t)\rangle. \tag{23}$$

Using the procedure analogous with SLF, one obtains

$$\langle\xi^2(t)_CD_0^\mu v(t)\rangle = e^{-\lambda t}\,_CD_0^\mu[\langle\xi^2(t)v(t)\rangle - 2qa^2\langle v(t)\rangle e^{\lambda t}] + 2qa^2\,_CD_0^\mu\langle v(t)\rangle, \tag{24}$$

and

$$\langle\xi^2(t)_CD_0^\nu x(t)\rangle = e^{-\lambda t}\,_CD_0^\nu[\langle\xi^2(t)x(t)\rangle - 2qa^2\langle x(t)\rangle e^{\lambda t}] + 2qa^2\,_CD_0^\nu\langle x(t)\rangle. \tag{25}$$

Considering the fact that in Equation (23) there is a new correlator $\langle\xi^2(t)v(u)\rangle$, we take the generalized Shapiro–Loginov procedure again, and we have

$$\langle\xi^2(t)v(u)\rangle = 2qa^2\langle v(u)\rangle + (\langle\xi^2(u)v(u)\rangle - 2qa^2\langle v(u)\rangle)e^{-\lambda(t-u)}. \tag{26}$$

$X_1(s)$, $X_2(s)$, $X_3(s)$, $X_4(s)$, $X_5(s)$, $X_6(s)$ are assumed to be LT of $\langle x \rangle$, $\langle v \rangle$, $\langle \xi x \rangle$, $\langle \xi v \rangle$, $\langle \xi^2 x \rangle$, $\langle \xi^2 v \rangle$, respectively. The initial values will vanish ($t \to \infty$). Using Equations (21), (22), (24)–(26), we can obtain the following results after LT:

$$
\begin{aligned}
&(s+\lambda)^\mu X_4(s) + [s^\mu + \hat{\gamma}(s)]X_2(s) + \omega_0^2[x_1(s) + X_3(s)] = \frac{A_0 s}{s^2 + \Omega^2}, \\
&s^\nu X_1(s) = X_2(s), \\
&(s+\lambda)^\mu X_6(s) + [(s+\lambda)^\mu + \hat{\gamma}(s+\lambda)]X_4(s) + \omega_0^2[X_3(s) + X_5(s)] \\
&\quad + 2qa^2[s^\mu - (s+\lambda)^\mu]X_2(s) = 0, \\
&(s+\lambda)^\nu X_3(s) = X_4(s), \\
&[(s+\lambda)^\mu + \hat{\gamma}(s+\lambda)]X_6(s) + a^2(s+\lambda)^\mu X_4(s) + \omega_0^2[X_5(s) + a^2 X_3(s)] \\
&\quad + 2qa^2[s^\mu - (s+\lambda)^\mu + \hat{\gamma}(s) - \hat{\gamma}(s+\lambda)]X_2(s) = 2qa^2 \frac{A_0 s}{s^2 + \Omega^2}, \\
&(s+\lambda)^\nu X_5(s) + 2qa^2[s^\nu - (s+\lambda)^\nu]x_1(s) = X_6(s),
\end{aligned}
\tag{27}
$$

in which $\hat{\gamma}(s)$ is LT of $\gamma(t)$,

$$
\hat{\gamma}(s) = \bar{\gamma} \frac{s^{\alpha\delta - \beta}}{(s^\alpha + \tau^{-\alpha})^\delta},
\tag{28}
$$

where $\bar{\gamma} = \frac{C_0}{\kappa_B T \tau^{\alpha\delta}}$. Solving of Equation (27), one can obtain

$$
X_1(s) = \frac{G(s)}{H(s)} \frac{A_0 s}{s^2 + \Omega^2},
\tag{29}
$$

where

$$
\begin{aligned}
G(s) &= [\hat{\gamma}(s+\lambda)(s+\lambda)^\nu + (s+\lambda)^{\mu+\nu} + \omega_0^2]^2 + (2q-1)a^2[(s+\lambda)^{\mu+\nu} + \omega_0^2]^2, \\
H(s) &= \{[\hat{\gamma}(s+\lambda)(s+\lambda)^\nu + (s+\lambda)^{\mu+\nu} + \omega_0^2]^2 - a^2[(s+\lambda)^{\mu+\nu} + \omega_0^2]^2\}[s^{\mu+\nu} + s^\nu\hat{\gamma}(s) + \omega_0^2] \\
&\quad + 2qa^2[(s+\lambda)^{\mu+\nu} + \hat{\gamma}(s+\lambda)(s+\lambda)^\nu + \omega_0^2][(s+\lambda)^{\mu+\nu} - s^{\mu+\nu}][(s+\lambda)^{\mu+\nu} + \omega_0^2] \\
&\quad + 2qa^2[s^\nu\hat{\gamma}(s) - \hat{\gamma}(s+\lambda)(s+\lambda)^\nu + s^{\mu+\nu} - (s+\lambda)^{\mu+\nu}][(s+\lambda)^{\mu+\nu} + \omega_0^2]^2.
\end{aligned}
\tag{30}
$$

For the stability of the solution conditions, it is necessary to assume that the following inequality holds:

$$
a^2 < [\lambda^{\mu+\nu} + \omega_0^2 + \bar{\gamma}\frac{\lambda^{\alpha\delta-\beta+\nu}}{(\lambda^\alpha + \tau^{-\alpha})^\delta}]^2 \{(\lambda^{\mu+\nu} + \omega_0^2)[\lambda^{\mu+\nu} + \omega_0^2 + 2q\bar{\gamma}\frac{\lambda^{\alpha\delta-\beta+\nu}}{(\lambda^\alpha + \tau^{-\alpha})^\delta}]\}^{-1}. \tag{31}
$$

Applying the linear response theory, we can yield the system stationary state response

$$
\langle x(t) \rangle_{as} = \lim_{t \to \infty} \langle x(t) \rangle = R \cos(\Omega t + \psi),
\tag{32}
$$

in which the output amplitude and phase shift are, respectively, given by

$$
R = A_0 \sqrt{\frac{f_1^2 + f_2^2}{f_3^2 + f_4^2}}, \psi = \arctan(\frac{f_2 f_3 - f_1 f_4}{f_1 f_3 + f_2 f_4}),
\tag{33}
$$

in which the related coefficients are given by

$$
\begin{aligned}
f_1 &= (c_1 + f_5 + \omega_0^2)^2 - (c_2 + f_6)^2 + (2q-1)a^2\{(\lambda^2 + \Omega^2)^{\mu+\nu}\cos[2\theta(\mu+\nu)] + \omega_0^4 + 2\omega_0^2 c_1\}, \\
f_2 &= 2(c_1 + f_5 + \omega_0^2)(c_2 + f_6) + (2q-1)a^2\{(\lambda^2 + \Omega^2)^{\mu+\nu}\sin[2\theta(\mu+\nu)] + 2\omega_0^2 c_2\}, \\
f_3 &= 2qa^2\{(c_1 + f_5 + \omega_0^2)(c_1 - c_3)(c_1 + \omega_0^2) - (c_2 + f_6)(c_2 - c_4)(c_1 + \omega_0^2) \\
&\quad - c_2(c_1 + f_5 + \omega_0^2)(c_2 - c_4) - c_2(c_2 + f_6)(c_1 - c_3) \\
&\quad + (c_3 - c_1 + f_7 - f_5)[(c_1 + \omega_0^2)^2 - c_2^2] - 2c_2(c_4 - c_2 + f_8 - f_6)(c_1 + \omega_0^2)\} \\
&\quad + [(c_1 + f_5 + \omega_0^2)^2 - (c_2 + f_6)^2 - a^2(c_1 + \omega_0^2)^2 + a^2 c_2^2](c_3 + f_7 + \omega_0^2) \\
&\quad - 2[(c_1 + f_5 + \omega_0^2)(c_2 + f_6) + c_2(c_1 + \omega_0^2)](c_4 + f_8), \\
f_4 &= 2qa^2\{c_2(c_1 + f_5 + \omega_0^2)(c_1 - c_3) - c_2(c_2 + f_6)(c_2 - c_4) \\
&\quad + (c_1 + f_5 + \omega_0^2)(c_2 - c_4)(c_1 + \omega_0^2) + (c_2 + f_6)(c_1 - c_3)(c_1 + \omega_0^2) \\
&\quad + 2c_2(c_3 - c_1 + f_7 - f_5)(c_1 + \omega_0^2) + (c_4 - c_2 + f_8 - f_6)[(c_1 + \omega_0^2)^2 - c_2^2]\} \\
&\quad + [(c_1 + f_5 + \omega_0^2)^2 - (c_2 + f_6)^2 - a^2(c_1 + \omega_0^2)^2 + a^2 c_2^2](c_4 + f_8) \\
&\quad + 2[(c_1 + f_5 + \omega_0^2)(c_2 + f_6) + c_2(c_1 + \omega_0^2)](c_3 + f_7 + \omega_0^2),
\end{aligned}
$$

$$
\begin{aligned}
f_5 &= \frac{\bar{\gamma}(\lambda^2 + \Omega^2)^{\frac{\alpha\delta - \beta + \nu}{2}}\cos[\theta(\alpha\delta - \beta + \nu) - \varphi_2\delta]}{[(\lambda^2 + \Omega^2)^\alpha + \tau^{-2\alpha} + 2\tau^{-\alpha}(\lambda^2 + \Omega^2)^{\frac{\alpha}{2}}\cos(\theta\alpha)]^{\frac{\delta}{2}}}, \\[2mm]
f_6 &= \frac{\bar{\gamma}(\lambda^2 + \Omega^2)^{\frac{\alpha\delta - \beta + \nu}{2}}\sin[\theta(\alpha\delta - \beta + \nu) - \varphi_2\delta]}{[(\lambda^2 + \Omega^2)^\alpha + \tau^{-2\alpha} + 2\tau^{-\alpha}(\lambda^2 + \Omega^2)^{\frac{\alpha}{2}}\cos(\theta\alpha)]^{\frac{\delta}{2}}}, \\[2mm]
f_7 &= \frac{\bar{\gamma}\Omega^{\alpha\delta - \beta + \nu}\cos[\frac{\pi}{2}(\alpha\delta - \beta + \nu) - \varphi_3\delta]}{[\Omega^{2\alpha} + \tau^{-2\alpha} + 2\tau^{-\alpha}\Omega^\alpha\cos(\frac{\pi}{2}\alpha)]^{\frac{\delta}{2}}}, \quad f_8 = \frac{\bar{\gamma}\Omega^{\alpha\delta - \beta + \nu}\sin[\frac{\pi}{2}(\alpha\delta - \beta + \nu) - \varphi_3\delta]}{[\Omega^{2\alpha} + \tau^{-2\alpha} + 2\tau^{-\alpha}\Omega^\alpha\cos(\frac{\pi}{2}\alpha)]^{\frac{\delta}{2}}}, \\[2mm]
c_1 &= (\lambda^2 + \Omega^2)^{\frac{\nu+\mu}{2}}\cos[\theta(\nu+\mu)], c_2 = (\lambda^2 + \Omega^2)^{\frac{\nu+\mu}{2}}\sin[\theta(\nu+\mu)], \\[2mm]
c_3 &= \Omega^{\mu+\nu}\cos[\frac{\pi}{2}(\nu+\mu)], c_4 = \Omega^{\nu+\mu}\sin[\frac{\pi}{2}(\nu+\mu)], \\[2mm]
\theta &= \arctan\frac{\Omega}{\lambda}, \varphi_2 = \arctan\frac{(\lambda^2 + \Omega^2)^{\frac{\alpha}{2}}\sin(\alpha\theta)}{(\lambda^2 + \Omega^2)^{\frac{\alpha}{2}}\cos(\alpha\theta) + \tau^{-\alpha}}, \varphi_3 = \arctan\frac{\Omega^\alpha\sin(\frac{\pi}{2}\alpha)}{\Omega^\alpha\cos(\frac{\pi}{2}\alpha) + \tau^{-\alpha}}.
\end{aligned}
\tag{34}
$$

Furthermore, the exact expression of SPA of FGLE (16) can be written as

$$
\text{SPA} = \frac{R^2}{A_0^2} = \frac{f_1^2 + f_2^2}{f_3^2 + f_4^2}.
\tag{35}
$$

For $\xi(t) = 0$ in Equation (16), one can note that SPA in Equation (35) would recover to

$$
\text{SPA} = \frac{1}{[\Omega^{\mu+\nu}\cos(\frac{\pi}{2}(\mu+\nu)) + f_7 + \omega_0^2]^2 + [f_8 + \Omega^{\mu+\nu}\sin(\frac{\pi}{2}(\mu+\nu))]^2}.
\tag{36}
$$

5. Resonance Behavior of FGLE

5.1. GSR for FGLE Only Influenced by GML Noise

Although some properties of the FGLE with GML noise have been studied in some papers, the resonance behaviors of an FGLE only induced by GML noise involving three parameter requires further discussion. To begin with, we will study the mechanism of the SR phenomenon of the FGLE in Equation (36) absence $\xi(t)$, i.e., $\xi(t) = 0$. According to Equation (36), Figure 2 displays GSR behaviors for the FGLE, SPA versus α. In Figure 2a, SPA(α) displays one peak and one valley in each curve, which indicates that GSR [10] and reverse SR [36] take place. In Figure 2a, it is easy to see that, with the increase in β, the valley lifts and moves to the right. In Figure 2a, one can also find the peak appears in SPA(α) at the beginning, and decreases with β increasing. However, the peak appears in the left of SPA(α), and the right peak of SPA(α) disappears if β keeps increasing. In Figure 2b,

SPA(α) displays one valley for about $\delta < 1.4$, and SPA(α) displays one valley and one peak for $\delta > 1.4$. It is obviously seen from Figure 2b that the valley lifts and slightly moves to the left with δ increasing. Figure 2b also shows that the resonance peak moves to the left as δ increases.
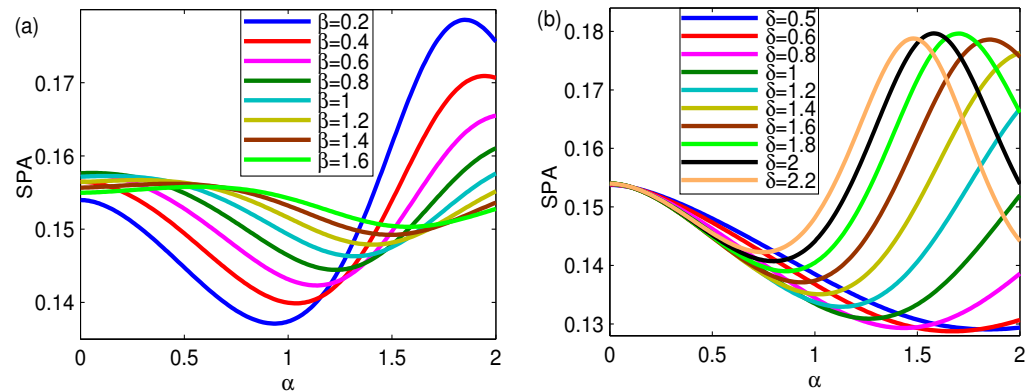
Figure 2. GSR behaviors of SPA(α) in (36) for different (**a**) β and (**b**) δ. (**a**) $\bar{\gamma} = 0.1$, $\delta = 1.6$, $\tau = 0.2$, $\omega_0 = 1$, $\Omega = 2$ $\mu = \nu = 0.9$; (**b**) $\bar{\gamma} = 0.1$, $\beta = 0.2$, $\tau = 0.2$, $\omega_0 = 1$, $\Omega = 2$, $\mu = \nu = 0.9$.

Figure 3 displays GSR for SPA in Equation (36) versus β. In Figure 3a, there is a peak in SPA(β) for about $\alpha < 0.9$, and SPA(β) exhibits a valley for $\alpha > 0.9$. Furthermore, in Figure 3a, the peak decreases as α increases. Then, the peak disappears while a valley emerges in its left side for α continues increasing. In Figure 3b, SPA(β) exhibits a valley in its left side for about $\tau < 0.2$, SPA(β) presents one peak and one valley for $0.2 < \tau < 0.8$, while SPA(β) exhibits a peak for about $\tau > 0.8$. Furthermore, in Figure 3b, the valley decreases and moves to the left until it vanishes as τ increases, while the resonance peak (if SPA(β) presents a peak) increases with τ increasing.
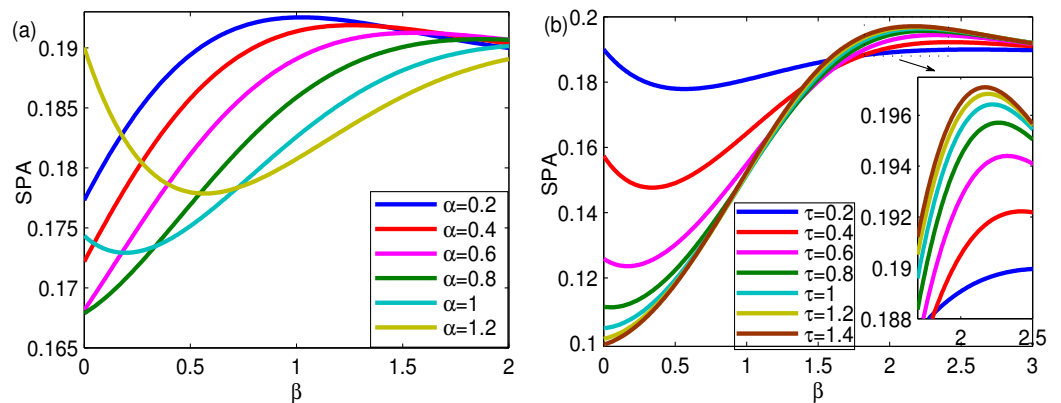
Figure 3. GSR behaviors of SPA(β) in (36) different (**a**) α and (**b**) τ. (**a**) $\bar{\gamma} = 0.1$, $\delta = 1.6$, $\tau = 0.2$, $\omega_0 = 1$, $\Omega = 2$, $\mu = \nu = 0.8$; (**b**) $\bar{\gamma} = 0.1$, $\alpha = 1.2$, $\delta = 1.6$, $\omega_0 = 1$, $\Omega = 2$, $\mu = \nu = 0.8$.

According to Equation (36), Figure 4 shows material resonance behaviors of SPA versus δ. Figure 4a depicts that SPA(δ) is monotonous for about $\alpha < 0.2$, SPA(δ) exhibits a valley for about $0.2 < \alpha < 0.6$, a peak and a valley exhibit in SPA(δ) for about $0.6 < \alpha < 1$, a peak and two valleys exhibit in SPA(δ) for about $1 < \alpha < 1.3$, and two or three peaks appear for about $\alpha > 1.4$. This phenomenon indicates that stochastic multi-resonance (SMR) phenomena occur [37]. Figure 4b presents a peak and two valleys that appear in SPA(δ). Figure 4b also demonstrates that the valleys lift, while the peak decreases with β increasing.
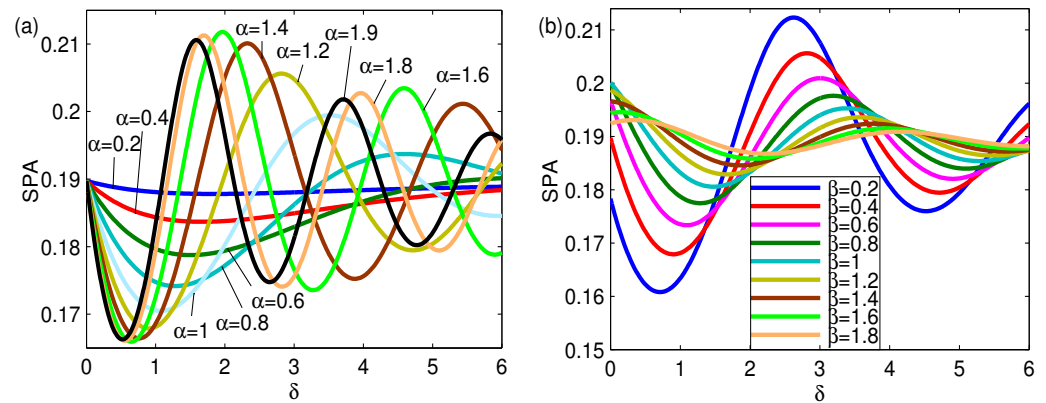
Figure 4. GSR behaviors of SPA(δ) in (36) for distinct (**a**) α and (**b**) β. (**a**) $\bar{\gamma} = 0.1$, $\beta = 0.4$, $\tau = 0.2$, $\omega_0 = 1$, $\Omega = 2$, $\mu = \nu = 0.8$; (**b**) $\bar{\gamma} = 0.1$, $\alpha = 1.2$, $\tau = 0.2$, $\omega_0 = 1$, $\Omega = 2$, $\mu = \nu = 0.8$.

5.2. GSR for FGLE Influenced by Two Types of Noise

It is interesting to discuss the resonance mechanism of the FGLE under synergy between multiplicative trichotomous noise and intrinsic additive noise with a three-parameter ML correlation function. In this subsection, according to Equation (35), we will address GSR for an FGLE influenced by two types of noise, $\xi(t)$ and $F(t)$. Figure 5 shows SPA versus α. As depicted in Figure 5a, a peak and a valley are seen in SPA(α), which indicates that GSR and reverse SR phenomena take place. Furthermore, in Figure 5a, the valley lifts; meanwhile, the peak decreases as β increases. It is obviously seen from Figure 5b that SPA(α) displays a valley and a flat resonance peak. Figure 5b also demonstrates that the valley lifts; meanwhile, the peak increases in parallel with q increasing, while the valley position and the peak position are almost unchanged.
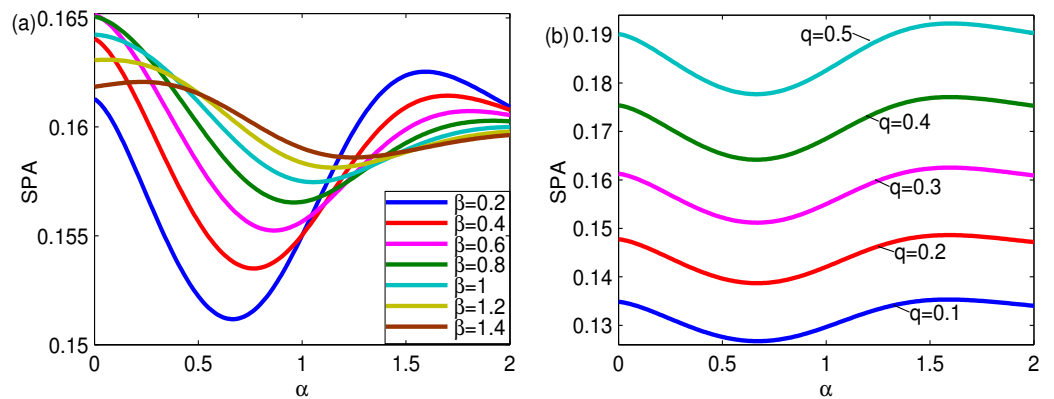
Figure 5. GSR behaviors of SPA(α) in (35) for different (**a**) β and (**b**) q. (**a**) $\bar{\gamma} = 0.1$, $\delta = 1.65$, $\tau = 0.1$, $a^2 = 0.2$, $q = 0.3$, $\lambda = 0.6$, $\omega_0 = 1$, $\Omega = 2$, $\mu = \nu = 0.8$; (**b**) $\beta = 0.2$, $\bar{\gamma} = 0.1$, $\delta = 1.65$, $\tau = 0.1$, $a^2 = 0.2$, $\lambda = 0.6$, $\omega_0 = 1$, $\Omega = 2$, $\mu = \nu = 0.8$.

Figure 6 shows GSR for SPA in Equation (35) versus β. In Figure 6a, SPA(β) presents a peak for about $\alpha < 0.9$, while SPA(β) displays a valley for about $\alpha > 0.9$. Figure 6a exhibits the peak decreases and moves to the right as α increases at the beginning. The peak disappears while a valley emerges; then, the valley lifts if α continues to increase. Figure 6b demonstrates that a peak appears in SPA(β) for about $\delta < 1$, while a valley appears in SPA(β) for about $\delta > 1$. Figure 6b also depicts that the peak decreases as δ increases at first. The peak disappears and a valley emerges in its left side; then, the valley lifts if δ continues increasing.
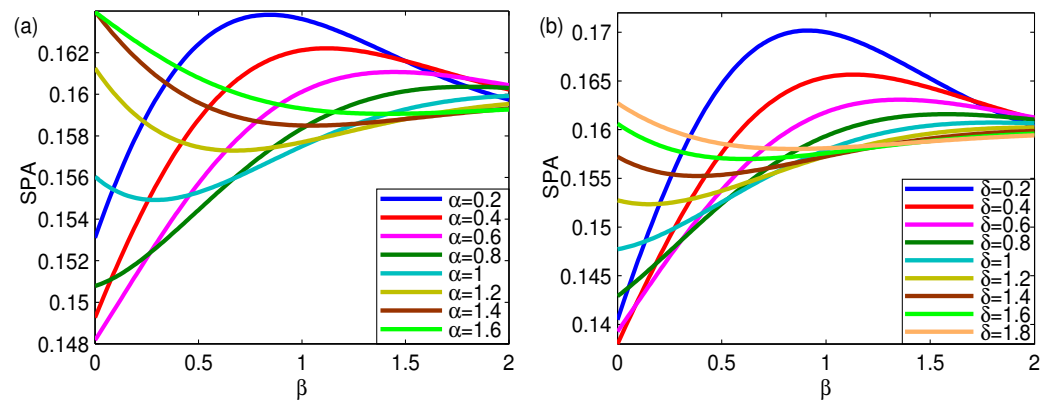
Figure 6. GSR behaviors of SPA(β) in (35) for different (**a**) α and (**b**) δ. (**a**) $\bar{\gamma} = 0.1$, $\delta = 1.65$, $\tau = 0.1$, $a^2 = 0.2$, $q = 0.3$, $\lambda = 0.6$, $\omega_0 = 1$, $\Omega = 2$, $\mu = \nu = 0.8$; (**b**) $\bar{\gamma} = 0.1$, $\alpha = 1.2$, $\tau = 0.1$, $a^2 = 0.2$, $q = 0.3$, $\lambda = 0.6$, $\omega_0 = 1$, $\Omega = 2$, $\mu = \nu = 0.8$.

Figure 7 demonstrates material resonance behaviors of SPA in Equation (35) versus δ. Figure 7a displays that SPA(δ) is monotonous for about $\alpha < 0.2$. Furthermore, a valley appears in SPA(δ) for about $0.2 < \alpha < 0.6$, while a peak and a valley appear in SPA(δ) for about $0.6 < \alpha < 1$, which means that the GSR phenomenon and reverse SR phenomenon take place, respectively. There are a peak and two valleys in SPA(δ) for about $1 < \alpha < 1.3$, and there are two or three peaks in the curve for about $\alpha \geq 1.4$, which means that SMR phenomena occur. Figure 7b plots that there are a peak and two valleys for about $\beta < 1$, and there are two peaks and a valley for about $\beta > 1$. Figure 7b also depicts that the valleys lift and the resonance peaks decrease as β increases.
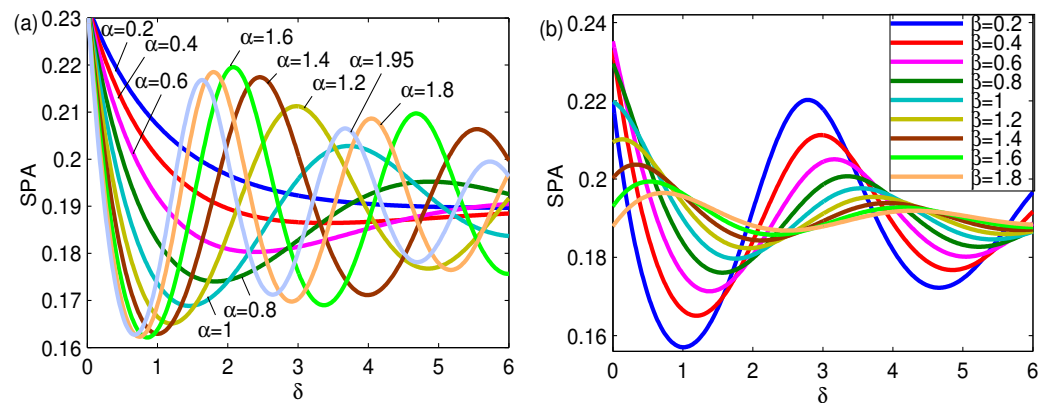
Figure 7. GSR behaviors of SPA(δ) in (35) for distinct (**a**) α and (**b**) β. (**a**) $\bar{\gamma} = 0.1$, $\beta = 0.4$, $\tau = 0.2$, $a^2 = 0.6$, $q = 0.3$, $\lambda = 0.6$, $\omega_0 = 1$, $\Omega = 2$, $\mu = \nu = 0.8$; (**b**) $\bar{\gamma} = 0.1$, $\alpha = 1.2$, $\tau = 0.2$, $a^2 = 0.2$, $q = 0.3$, $\lambda = 0.6$, $\omega_0 = 1$, $\Omega = 2$, $\mu = \nu = 0.8$.

Figure 8 depicts SPA with Equation (35) versus the fractional order μ. In Figure 8a, SPA(μ) exhibits a valley for about $\nu < 0.6$, which indicates that a reverse SR phenomenon takes place; SPA(μ) exhibits a resonance peak for about $\nu \geq 0.6$, which indicates that the GSR appears. Furthermore, in Figure 8a, the maximum increase and its position moves to the left as ν increases. As depicted in Figure 8b, a peak appears in SPA(μ) for various q and the peak increases, while its position remains almost unchanged as q increases.
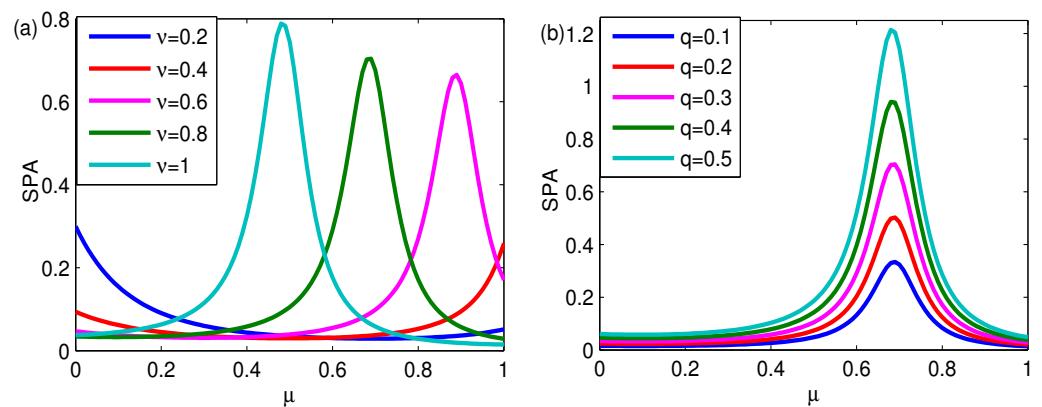
Figure 8. GSR behaviors of SPA(μ) in (35) for different (**a**) ν and (**b**) q. (**a**) $\bar{\gamma} = 0.1$, $\alpha = 1.2$, $\beta = 0.2$, $\delta = 1.6$, $\tau = 0.2$, $\lambda = 0.6$, $a^2 = 0.6$, $q = 0.3$, $\Omega = 2$, $\omega_0 = 1$; (**b**) $\nu = 0.8$, $\alpha = 1.2$, $\beta = 0.2$, $\bar{\gamma} = 0.1$, $\delta = 1.6$, $\tau = 0.2$, $\lambda = 0.6$, $a^2 = 0.6$, $\Omega = 2$, $\omega_0 = 1$.

Figure 9 exhibits GSR for SPA in Equation (35) versus the fractional order ν. In Figure 9a, a resonance peak appears in SPA(ν) for various τ and the maximum decreases; meanwhile, its position remains almost unchanged as τ increases. In Figure 9b, SPA(ν) exhibits a resonance peak for various λ, while the maximum decreases and moves to the right as λ increases.
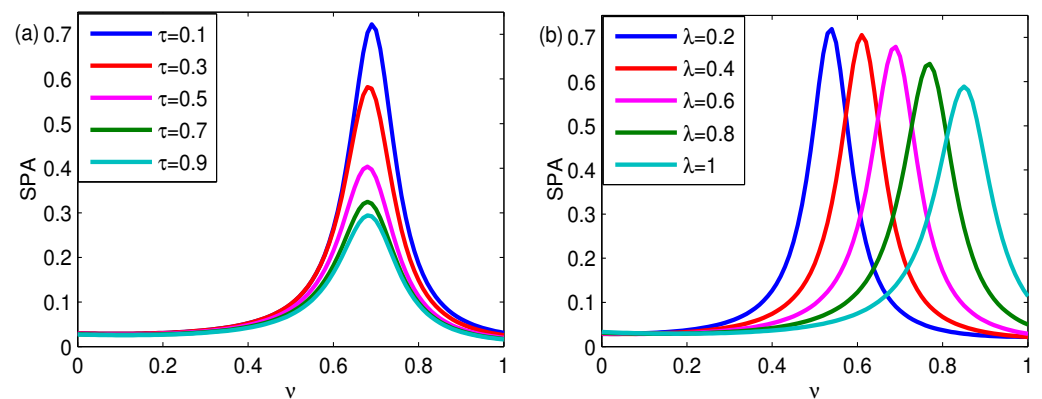
Figure 9. GSR behaviors of SPA(ν) in (35) for distinct (**a**) τ and (**b**) λ. (**a**) $\alpha = 1.2$, $\beta = 0.2$, $\bar{\gamma} = 0.1$, $\delta = 1.6$, $\mu = 0.8$, $a^2 = 0.6$, $\lambda = 0.6$, $q = 0.3$, $\omega_0 = 1$, $\Omega = 2$; (**b**) $\alpha = 1.2$, $\beta = 0.2$, $\bar{\gamma} = 0.1$, $\delta = 1.6$, $\mu = 0.8$, $\tau = 0.2$, $a^2 = 0.6$, $q = 0.3$, $\omega_0 = 1$, $\Omega = 2$.

Figure 10 displays the GSR for SPA with Equation (35) versus a^2. In Figure 10a, a peak appears in SPA(a^2) for various β, and the peak increases as β increases. Figure 10b shows that SPA(a^2) exhibits a peak for various τ, and the peak decreases and moves slightly to the right as τ increases.

Figure 11 presents GSR behaviors for SPA in Equation (35) versus λ. Figure 11a displays that SPA(λ) exhibits a resonance peak in for various τ. Furthermore, in Figure 11a, the peak decreases, while its position is almost unchanged as τ increases. In Figure 11b, SPA(λ) also exhibits a resonance peak for various q and the maximum increases, while its position is almost unchanged as q increases.
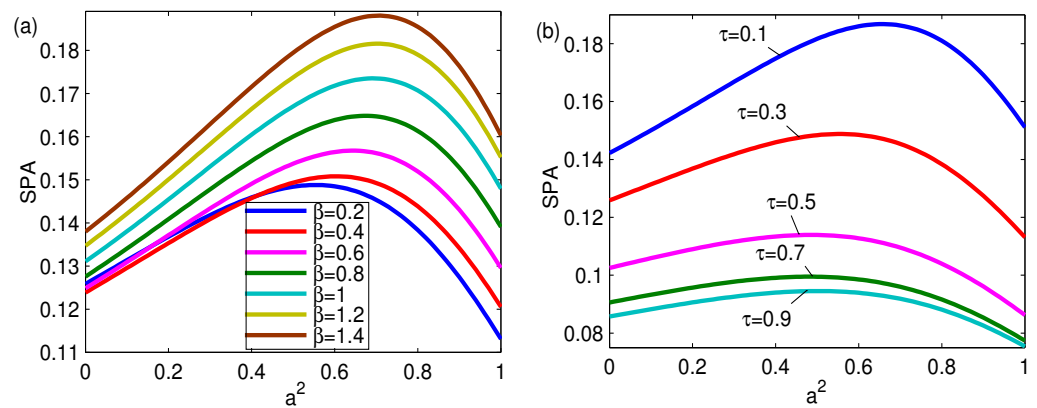
Figure 10. GSR behaviors of SPA(a^2) in (35) for different (**a**) β and (**b**) τ. (**a**) $\alpha = 1.2$, $\bar{\gamma} = 0.1$, $\delta = 1.6$, $\tau = 0.3$, $q = 0.3$, $\lambda = 0.6$, $\omega_0 = 1$, $\Omega = 2$, $\mu = \nu = 0.8$; (**b**) $\alpha = 1.2$, $\beta = 0.2$, $\bar{\gamma} = 0.1$, $\delta = 1.6$, $q = 0.3$, $\lambda = 0.6$, $\omega_0 = 1$, $\Omega = 2$, $\mu = \nu = 0.8$.
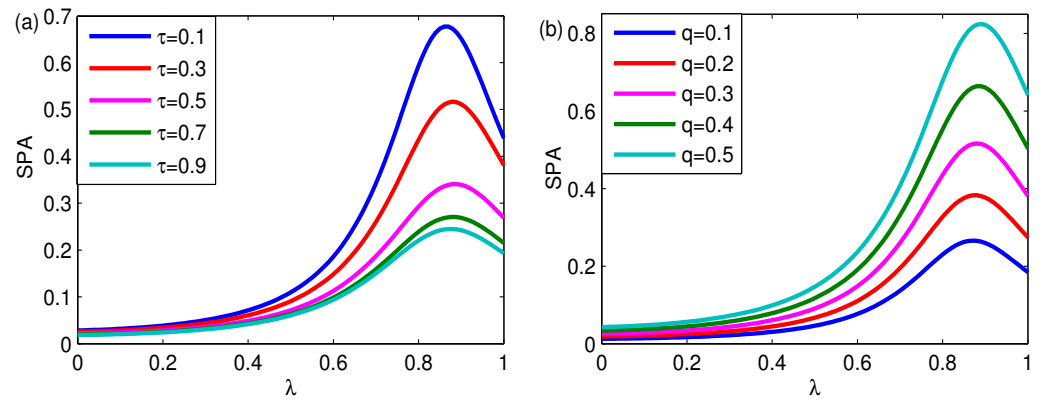
Figure 11. GSR behaviors of SPA(λ) in (35) for distinct (**a**) τ and (**b**) q. (**a**) $\alpha = 1.2$, $\beta = 0.2$, $\bar{\gamma} = 0.1$, $\delta = 1.6$, $a^2 = 0.6$, $q = 0.3$, $\omega_0 = 1$, $\Omega = 2$, $\mu = \nu = 0.8$; (**b**) $\alpha = 1.2$, $\beta = 0.2$, $\bar{\gamma} = 0.1$, $\delta = 1.6$, $\tau = 0.3$, $a^2 = 0.6$, $\omega_0 = 1$, $\Omega = 2$, $\mu = \nu = 0.8$.

6. Summary

To conclude, in this work we have explored the GSR behaviors of an FGLE with fluctuating mass, fluctuating frequency, and GML noise involving three parameters. One of the main parts of our work is that the noise spectral of the GML noise involving three parameters has been discussed. By using the LT technique, the exact expression of SPA of the FGLE has been found. The various resonance behaviors of SPA have been extensively studied. Importantly, some results of significance are found. For instance, the GSR, reverse SR phenomenon, and SMR phenomena have been found. Furthermore, there are some results that could be deserved as follows.

(i) GSR for the FGLE could be only influenced by GML noise involving three parameters. GSR and reverse SR could be observed in the behavior of SPA only under the effect of GML noise. In particular, SMR can only be influenced by the parameter δ of GML noise.

(ii) GSR for the FGLE could be influenced by two types of noise. Resonance behaviors of the FGLE under the synergy between extrinsic multiplicative noise and GML noise maintain the GSR behaviors of the FGLE. In addition, the parameters a^2, λ, and q of multiplicative noise could induce the GSR phenomenon.

(iii) The GSR phenomenon could be induced by the fractional orders μ or ν of the FGLE. It could be found that GSR phenomena in the FGLE have many more material results than GSR in GLE.

Refs. [27–29,34] mainly focused on anomalous diffusion phenomena, which were described by the FGLE with various types of ML noise or GML noise. In some special background, fluctuating parameters may also influence the physical performance of the

systems. In this work, GSR induced by fluctuating parameters together with thermal noise, which was described by a GML noise, has been addressed. Ref. [12] studied the FGLE with random frequency and a two-parameter GML noise. Different from previous studies, the main contribution of this work is the investigation of various behaviors of GSR influence by random mass, random frequency, and a three-parameter GML noise.

On account of three-parameter ML noise involving different kinds of noise, three-parameter ML noise can be used to describe anomalous dielectrics, disturbance of the electron temperature and density, disordered materials, and heterogeneous systems. Moreover, it has been proved that the FGLE is suitable for characterizing various anomalous diffusion phenomena. Thus, we believe that our work presents theoretical significance for diffusion theory, and it also provides applications for plasma physics, as well as mechanical and electrical engineering.

Author Contributions: Conceptualization, G.H. and L.Q.; methodology, G.H. and L.Q.; software, L.Q. and Y.P.; validation, L.Q., H.C. and Y.T.; formal analysis, G.H. and L.Q.; investigation, G.H. and L.Q.; resources, L.Q.; data curation, L.Q. and Y.P.; writing—original draft preparation, G.H., L.Q., Y.P., H.C. and Y.T.; writing—review and editing, L.Q.; visualization, L.Q.; supervision, G.H.; project administration, G.H.; funding acquisition, G.H. All authors have read and agreed to the published version of the manuscript.

Institutional Review Board Statement: Not applicable.

Informed Consent Statement: Not applicable.

Data Availability Statement: Not applicable.

Conflicts of Interest: The authors declare no conflict of interest.

References

1. Benzi, R.; Sutera, A.; Vulpiani, A. The mechanism of stochastic resonance. *J. Phys. A Math. Gen.* **1981**, *14*, L453. [CrossRef]
2. Benzi, R. Stochastic resonance: From climate to biology. *Nonlinear Process. Geophys.* **2010**, *17*, C431–C441. [CrossRef]
3. Gammaitoni, L.; Hänggi, P.; Jung, P.; Marchesoni, F. Stochastic resonance: A remarkable idea that changed our perception of noise. *Eur. Phys. J. B* **2009**, *69*, 1–3. [CrossRef]
4. Falanga, M.; De Lauro, E.; de Martino, S. Stochastic resonance observed in aerosol optical depth Time Series. *Atmosphere* **2020**, *11*, 502. [CrossRef]
5. McDonnell, M.D.; Stocks, N.G.; Pearce, C.E.M.; Abbott, D. *Stochastic Resonance*; Cambridge University Press: Cambridge, UK, 2008.
6. Ren, R.; Yuan, G.X. Collective behaviors of star-coupled harmonic oscillators with fluctuating frequency in the presence of stochastic resonance. *Fractal Fract.* **2022**, *6*, 414. [CrossRef]
7. Huang, W.; Zhang, G.; Jiao, S.; Wang, J. Bearing fault diagnosis based on stochastic resonance and improved whale optimization algorithm. *Electronics* **2022**, *11*, 2185. [CrossRef]
8. Yang, Z.; Li, Z.; Zhou, F.; Ma, Y.; Yan, B. Weak fault feature extraction method based on improved stochastic resonance. *Sensors* **2022**, *22*, 6644. [CrossRef]
9. Lu, S.L.; He, Q.B.; Hu, F.; Kong, F.R. Sequential multiscale noise tuning stochastic resonance for train bearing fault diagnosis in an embedded system. *IEEE Trans. Instru. Meas.* **2014**, *63*, 106. [CrossRef]
10. Gitterman, M. Classical harmonic oscillator with multiplicative noise. *Phys. A* **2005**, *352*, 309. [CrossRef]
11. Bobryk, R.V. Stochastic multiresonance in oscillators induced by bounded noise. *Commun. Nonlin. Sci. Numer. Simul.* **2021**, *93*, 105460. [CrossRef]
12. He, G.; Tian, Y.; Luo, M. Mittag–Leffler noise induced resonance behavior in a fractional generalized Langevin equation with random trichotomous inherent frequency. *J. Stat. Mech.* **2018**, *2018*, 033201. [CrossRef]
13. He, G.; Liu, H.; Tang, G.J.; Cao, J.D. Resonance behavior for a generalized Mittag–Leffler fractional Langevin equation with hydrodynamic interactions. *Int. J. Mode. Phys. B* **2020**, *34*, 2050310. [CrossRef]
14. Burov, S.; Barkai, E. Fractional Langevin equation: Overdamped, underdamped, and critical behaviors. *Phys. Rev. E* **2008**, *78*, 031112. [CrossRef] [PubMed]

15. Soika, E.; Mankin, R.; Ainsaar, A. Resonant behavior of a fractional oscillator with fluctuating frequency. *Phys. Rev. E* **2010**, *81*, 011141. [CrossRef]
16. Ghosh, S.K.; Cherstvy, A.G.; Grebenkov, D.S.; Grebenkov, D.S.; Metzler, R. Anomalous, non-Gaussian tracer diffusion in crowded two-dimensional environments. *New J. Phys.* **2016**, *18*, 013027. [CrossRef]
17. Méndez, V.D.; Campos, F. *Stochastic Foundations in Movement Ecology*; Springer: Berlin, Germany, 2016.
18. Goychuk, I.; Kharchenko, V. Fractional Brownian motors and stochastic resonance. *Phys. Rev. E* **2012**, *85*, 051131. [CrossRef]
19. Kubo, R. The fluctuation-dissipation theorem. *Rep. Prog. Phys.* **1966**, *29*, 255. [CrossRef]
20. Grebenkov, D.S.; Vahabi, M. Analytical solution of the generalized Langevin equation with hydrodynamic interactions: Subdiffusion of heavy tracers. *Phys. Rev. E* **2014**, *89*, 012130. [CrossRef] [PubMed]
21. Kilbas, A.A.; Sarivastava, H.M.; Trujillo, J.J. *Theory and Applications of Fractional Differential Equations*; Elsevier: New York, NY, USA, 2006.
22. Mainardi, F.; Pironi, P. The fractional Langevin equation: Brownian motion revisited. *Extr. Math.* **1996**, *10*, 140–154.
23. Lim, S.C.; Teo, L.P. Modeling single-file diffusion with step fractional Brownian motion and a generalized fractional Langevin equation. *J. Stat. Mech.* **2009**, *2009*, P08015. [CrossRef]
24. Eab, C.H.; Lim, S.C. Fractional generalized Langevin equation approach to single-file diffusion. *Phys. A* **2010**, *389*, 2510–2521. [CrossRef]
25. Li, H.L.; He, G.T.; Peng, Y.; Cheng, H. Stochastic resonance for a Jerk oscillator with a generalized Mittag–Leffler noise. *Chin. J. Phys.* **2022**, *77*, 1997–2013. [CrossRef]
26. Viñales, A.D.; Despósito, M.A. Anomalous diffusion induced by a Mittag–Leffler correlated noise. *Phys. Rev. E* **2007**, *75*, 042102. [CrossRef] [PubMed]
27. Figueiredo, C.R.; Capelas de Oliveira, E.; Vaz, J.J. On anomalous diffusion and the fractional generalized Langevin equation for a harmonic oscillator. *J. Math. Phys.* **2009**, *50*, 123518. [CrossRef]
28. Fa, K.S. Anomalous diffusion in a generalized Langevin equation. *J. Math. Phys.* **2009**, *50*, 083301. [CrossRef]
29. Sandev, T.; Metzler, R.; Tomovski, Ž. Velocity and displacement correlation functions for fractional generalized Langevin equations. *Fract. Calc. Appl. Anal.* **2012**, *15*, 426–450. [CrossRef]
30. Prabhakar, T.R. A singular integral equation with a generalized Mittag–Leffler function in the kernel. *Yokohama Math. J.* **1971**, *19*, C7–C15.
31. Marchesoni, F. Comment on stochastic resonance in washboard potentials. *Phys. Lett. A* **1997**, *231*, 61–64. [CrossRef]
32. Gitterman, M. Stochastic oscillator with random mass: New type of Brownian motion. *Phys. A* **2014**, *395*, 11–21. [CrossRef]
33. Mankin, R.; Laas, K.; Laas, T. Stochastic multiresonance and correlation-time-controlled stability for a harmonic oscillator with fluctuating frequency. *Phys. Rev. E* **2008**, *78*, 031120. [CrossRef]
34. Pottier, N. Relaxation time distributions for an anomalously diffusing particle. *Phys. A* **2011**, *390*, 2863–2879. [CrossRef]
35. Shapiro, V.E.; Loginov, V.M. "Formulae of differentiation" and their use for solving stochastic equations. *Phys. A* **1978**, *91*, 563–574. [CrossRef]
36. Li, J.C.; Mei, D.C. Reverse resonance in stock prices of financial system with periodic information. *Phys. Rev. E* **2013**, *88*, 012811. [CrossRef] [PubMed]
37. Vilar, J.M.G.; Rubi, J.M. Stochastic multiresonance. *Phys. Rev. Lett.* **1997**, *78*, 2882. [CrossRef]